

Effect of hydrophobic environments on the hypothesized liquid-liquid critical point of water

Elena G. Strekalova · Dario Corradini ·
Marco G. Mazza · Sergey V. Buldyrev · Paola Gallo ·
Giancarlo Franzese · H. Eugene Stanley

Received: 19 May 2011 / Accepted: 27 September 2011
© Springer Science+Business Media B.V. 2011

Abstract The complex behavior of liquid water, along with its anomalies and their crucial role in the existence of life, continue to attract the attention of researchers. The anomalous behavior of water is more pronounced at subfreezing temperatures and numerous theoretical and experimental studies are directed towards developing a coherent thermodynamic and dynamic framework for understanding supercooled water. The existence of a liquid–liquid critical point in the deep supercooled region has been related to the anomalous behavior of water. However, the experimental study of supercooled water at very low temperatures is hampered by the homogeneous nucleation of the crystal. Recently, water confined in nanoscopic structures or in solutions has attracted interest because nucleation can be delayed. These systems have a tremendous relevance also for current biological advances; e.g., supercooled water is often confined in cell membranes and acts as a solvent for biological molecules. In particular, considerable attention has been recently devoted to understanding hydrophobic interactions or the behavior of water in the presence of apolar interfaces due to their fundamental role in self-assembly of micelles, membrane formation and

E. G. Strekalova (✉) · D. Corradini · H. E. Stanley
Center for Polymer Studies and Department of Physics,
Boston University, Boston, MA 02215, USA
e-mail: elena@buphy.bu.edu

M. G. Mazza
Stranski-Laboratorium für Physikalische und Theoretische Chemie,
Technische Universität Berlin, Straße des 17. Juni 135, 10623 Berlin, Germany

S. V. Buldyrev
Department of Physics, Yeshiva University, 500 West 185th Street, New York, NY 10033, USA

P. Gallo
Dipartimento di Fisica, Università Roma Tre, Via della Vasca Navale 84, I-00146 Roma, Italy

G. Franzese
Departament de Física Fonamental, Universitat de Barcelona,
Diagonal 645, 08028 Barcelona, Spain

protein folding. This article reviews and compares two very recent computational works aimed at elucidating the changes in the thermodynamic behavior in the supercooled region and the liquid–liquid critical point phenomenon for water in contact with hydrophobic environments. The results are also compared to previous reports for water in hydrophobic environments.

Keywords Water · Hydrophobic · Confinement · Solutions · Simulations

PACS 64.70.Ja · 65.20.-w · 66.10.C-

1 Introduction

We often think of water as a typical liquid because of its ubiquity in our lives. However, the thermodynamic behavior of water is very complex and anomalous when compared to simple liquids [1, 2]. Its isothermal compressibility, isobaric specific heat, and coefficient of thermal expansion, in fact, show a non-monotonic behavior, displaying an apparent divergence in the supercooled region [3, 4]. Moreover, water presents a density anomaly, i.e., a decrease in density upon isobaric cooling [5]. The border of the region of density anomaly is marked by the temperature of maximum density (TMD) line.

To explain the anomalous behavior of water, in 1992 the *liquid–liquid critical point scenario* was hypothesized for supercooled water [6]. Since then, several computer simulations have modeled a singular behavior for supercooled water, i.e., the appearance of a liquid–liquid critical point (LLCP) at the end of a liquid–liquid phase transition (LLPT) line between two types of liquid water, high-density liquid (HDL) and low-density liquid (LDL) [7–14].

The experimental study of water in the supercooled region, where its anomalies are more pronounced, is extremely difficult due the homogeneous nucleation of the crystal phase, occurring at $T = 235$ K at ambient pressure [1]. One way to explore this experimentally unaccessible region is to nanoconfine water, which forces it to remain in the liquid phase at temperatures where bulk water freezes, and a number of recent studies of the behavior of supercooled water have utilized various confining geometries, such as slits, pores or porous media [15–29].

The study of confined water at low temperatures is relevant to a wide range of fields, including food refrigeration and the cryopreservation of, for example, stem cells, umbilical cord blood, and embryos. In both refrigeration and cryopreservation, extracellular or intracellular ice formation, dehydration, and solute concentration due to ice crystal growth can permanently damage cells but, under the proper conditions, this destructive phenomenon can be inhibited through the use of confinement techniques [30–34].

Another way to extend the accessible region in supercooled water is to investigate aqueous solutions, because the homogeneous nucleation temperature of water often decreases in temperature when solutes are added [35]. Several recent studies have explored supercooled water in aqueous solutions of hydrophilic [36–43] and hydrophobic solutes [44, 45]. The properties of supercooled aqueous solutions are relevant to many biological and geophysical systems and, in particular, are of great interest when cryopreserving biological tissues [46].

Of particular interest is the behavior of water in contact with apolar surfaces or with apolar solutes. The study of water in these hydrophobic environments helps us understand such diverse phenomena as biological membrane formation, surfactant micellization, the

folding of globular proteins, and the stability of mesoscopic assemblies [47–49]. Thus, understanding how hydrophobic interfaces and solutes affect the thermodynamics of supercooled liquid water also helps us understand the biology and biophysics of life under subfreezing conditions. In such studies, the crucial question to ask is how water in the hydrophobic environment differs from bulk water. One way to approach this fundamental question is to perform computer simulations. Recent simplified models, such as 2D square lattice models or 3D spherically symmetric potentials with two length scales, have captured the anomalous behavior of water, including the appearance of a LLPT ending in a LLCP [50–53].

In this paper, we review how hydrophobic particles affect the thermodynamic behavior of supercooled liquid water. In particular, we discuss and compare the results obtained for hydrophobic objects in a 2D square lattice model for water, studied using Monte Carlo (MC) simulations [25] and the results obtained for mixtures of hard spheres (HS) and Jagla ramp potential particles studied using discrete molecular dynamics (DMD) simulations [44]. These results are then compared to previous observations for water in hydrophobic environments at subfreezing temperatures [26, 28, 29, 45, 54, 55].

The paper is organized as follows. Section 2 outlines the details of the models used in our computer simulations [25, 44]. Section 3 reviews the recent findings reported in these computational studies. The results are compared to previous reports for supercooled water in hydrophobic environments in Section 4. Conclusions are discussed in Section 5.

2 Models and simulation details

2.1 MC simulations of a coarse-grained model of water confined in a matrix of hydrophobic particles

The MC method is a computational tool that allows us to simulate the random thermal fluctuations of a system by sampling its different states at equilibrium. Different algorithms have been developed to optimize the MC simulation of spin models and cell models [56, 57]. The Wolff cluster algorithm [58] has become a particularly useful tool for the simulation of water when coarse-grained or cell models are utilized [53, 59–61].

Here we review MC simulations performed in the *NPT* ensemble on a water monolayer between two hydrophobic extended flat surfaces separated by about 0.7 nm, partitioned into \mathcal{N} cells, each with four nearest neighbors (n.n.). Each cell is occupied either by a water molecule or a hydrophobic nanoparticle whose size is controlled by the number of cells it occupies. The nanoparticles have an approximately spherical shape and are randomly distributed to form a fixed matrix that mimics a porous system or a rough atomic interface. Each water cell has four bond indices with q orientations that determine whether a hydrogen bond (HB) can be formed between the n.n. We choose q possible orientational states based on the assumption that the HB breaks when its angle deviation exceeds $\pm 30^\circ$, therefore $q = 360/60 = 6$. The model incorporates isotropic interactions, the HB directional two-body interaction, and the HB many-body interaction. In addition, the model takes into account the restructuring effect of water in the first hydration shell by explicitly increasing the strength of the HB by 30%. The coarse-grained model employed in this simulation in the absence of hydrophobic interfaces has been extensively explored and has reproduced the thermodynamic anomalies of water and has predicted a first-order LLPT and the LLCP

[14, 59, 60, 62–69]. Furthermore, the model allows to explain the observed phase transition in terms of the proliferation of regions with tetrahedrally ordered molecules.

Using MC simulations, we investigated system sizes up to $\mathcal{N} = 1.6 \times 10^5$ with nanoparticles of radius $R = 1.6$ nm for different concentrations $c \equiv (\mathcal{N} - N)/\mathcal{N}$ ranging from 2.4% to 25%, where N is the total number of water cells. The analysis was repeated for nanoparticles with $R = 0.4$ nm. A snapshot of this coarse-grained model of a water monolayer with hydrophobic nanoparticles of $R = 0.4$ nm and $c = 2.4\%$ is shown in Fig. 1(a).

2.2 DMD simulations on mixtures of Jagla ramp potential particles and hard spheres

DMD is a computer simulation method in which particles interact with discontinuous stepwise potentials. In DMD, particles move along straight lines with constant velocities until a collision, signaled by a discontinuity in the interaction potential, is encountered. After this event, the coordinates and velocities of the particles are updated. DMD is an efficient molecular dynamics (MD) technique, and, unlike the standard MD method, it allows us to easily simulate potentials containing hard cores. In a sense, DMD is equivalent to a Metropolis MC in which the set of moves is equivalent to the ballistic motion of the particles. As a result, DMD simulations are very efficient when studying polymers, colloids, and lipid membranes [70].

Over the last decade, several papers have shown that the presence of tetrahedrality or even of orientation-dependent interactions in computer models of water are not necessary conditions for the appearance of water anomalies or of a LLPT [51, 52, 71–88]. In fact, the

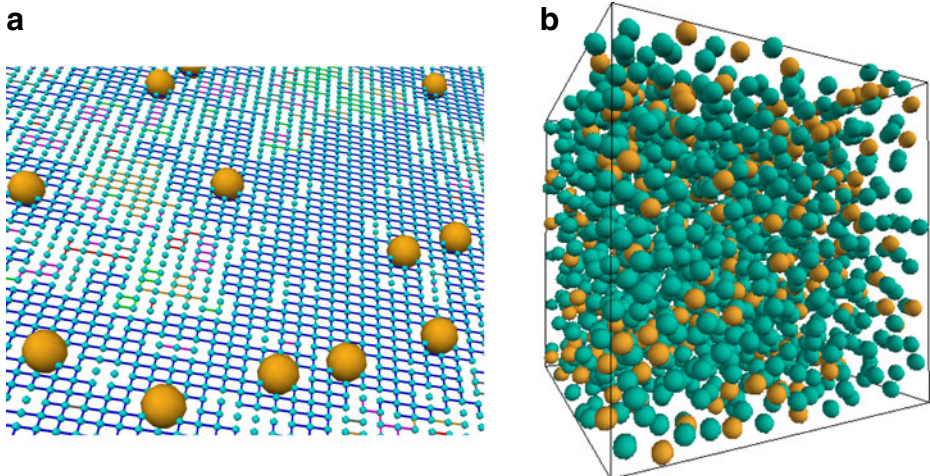


Fig. 1 **a** Snapshot of an equilibrated configuration for the water monolayer with randomly positioned fixed hydrophobic nanoparticles (*yellow spheres*) of radius $R = 0.4$ nm. Each water cell is represented by a small *cyan sphere*. *Colored lines* represent hydrogen bonds between molecules in nearest neighbor cells, with six possible colors corresponding to different possible bonding states. **b** Snapshot of an equilibrated configuration for the mixture of Jagla ramp particles (*green spheres*) and HS (*yellow spheres*) with HS mole fraction $x_{HS} = 0.20$. The total number of particles is 1728

Jagla potentials, a family of spherically symmetric potentials composed of a hard core and a linear repulsive ramp, can reproduce both water-like anomalies and the LLPT by tuning the ratio between the two characteristic lengths [89–93]. It has been suggested that the hard-core length corresponds to the first coordination shell of water molecules while the repulsive ramp length corresponds to the second coordination shell [91–93]. It is important to mention that Jagla potentials differ from water. In particular, the slope of the LLPT in the $P-T$ plane, related to the difference in entropy of HDL and LDL, in the Jagla potentials has an opposite sign with respect to water. It is therefore important to understand the consequences of the differing entropy behavior by comparing the results of the Jagla potentials with those of water-like models.

The investigated systems are mixtures of Jagla ramp particles and HS with identical diameters and the same mass m . The mole fractions studied spanned from $x_{\text{HS}} = 0.10$ to 0.50. A snapshot of the $x_{\text{HS}} = 0.20$ mixture is presented in Fig. 1(b).

In Fig. 2, the shape of the spherically symmetric Jagla ramp potential is shown. For the results we review, the Jagla potential was built considering a hard-core diameter a and a soft-core diameter, at the end of a linear repulsive ramp, b , where $b/a = 1.72$. The potential was supplemented with an attractive linear tail that extends to the cutoff $c = 3a$. The potential has been discretized, with the step $\Delta U = U_0/8$, where U_0 is the minimum of the energy that corresponds to the soft-core distance. The repulsive ramp was partitioned in 36 steps of width $0.02a$ and the attractive ramp into eight steps of width $0.16a$. The energy at the hard-core distance is defined as $U_R = 3.56 U_0$, the value of the least-squares linear fit of the discretized ramp at $r = a$. The systems were simulated at a constant number of particles, volume, and temperature. The temperature was controlled by a modified Berendsen algorithm [70]. For the DMD simulations, all quantities are expressed in reduced units: distances in units of a , energies in units of U_0 , times in units $a\sqrt{m/U_0}$, pressures in units of U_0/a^3 and temperatures in units of U_0/k_B . The density is defined as $\rho \equiv N/L^3$, with L the edge of the cubic simulation box, and is measured in units of a^{-3} . The total number of particles is $N = 1728$.

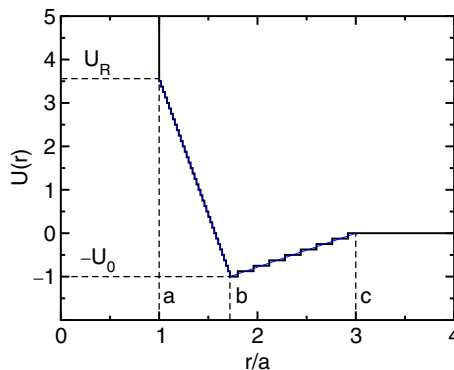


Fig. 2 Spherically symmetric Jagla ramp potential. Its two length scales correspond to the hard-core distance a and the soft-core distance b . The parameters of the potential studied were set to $b/a = 1.72$ and $U_R/U_0 = 3.56$. The potential was supplemented by an attractive tail and a long range cutoff was imposed at $c/a = 3$. The discretized version of the potential (see text) is shown (black solid line) along with the original continuous version (blue line)

3 The LLCP of water in hydrophobic environments

In this section, we present the results obtained in the MC simulations of the coarse-grained model of water confined in a hydrophobic matrix of particles and in the DMD simulations on mixtures of Jagla ramp potential particles and HS. There have been extensive computational studies of both approaches considered here without the addition of the hydrophobic particles [14, 51–53, 63–65, 94] that showed the presence of water anomalies, such as the density anomaly and peaks of the thermodynamic response functions. These studies were also consistent with the theoretical predictions of the existence of two types of liquids, i.e., LDL and HDL, in the subfreezing region of the $P - T$ phase diagram of liquid water, separated by a first-order LLPT and terminating with a LLCP. Here we show how the presence of hydrophobic particles affects the liquid–liquid phase diagram of water.

3.1 MC simulations on 2D water confined in a matrix of hydrophobic particles

Franzese et al. [14, 53, 59, 60, 63–69] previously showed that for $c = 0\%$ the coarse-grained model of a water monolayer employed here for the MC simulations captures the major thermodynamic phenomena of liquid water such as the liquid-gas spinodal, the locus of density maxima, the diffusion anomaly, and a first-order LLPT line that terminates in a LLCP at about 174 K and 0.13 GPa (Fig. 3). When we added a fixed matrix of hydrophobic

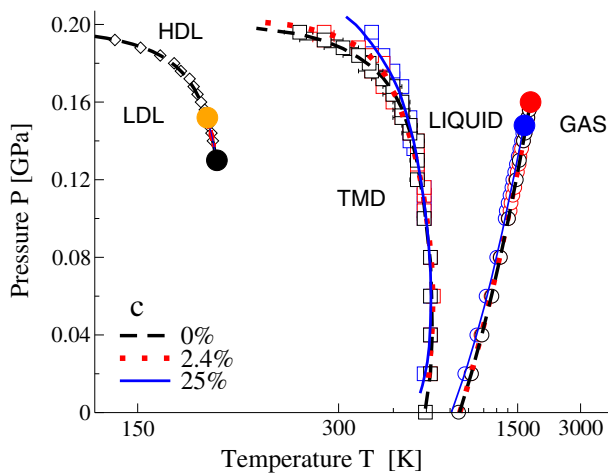


Fig. 3 $P - T$ phase diagram for the water coarse-grained model at different nanoparticle concentrations c , obtained by MC simulations. The T axis is shown in logarithmic scale. The liquid-gas spinodal is denoted by open circles, the TMD line by open squares, and the liquid-liquid spinodal by open diamonds. Lines are guides for the eyes (dashed for $c = 0\%$, dotted for 2.4% and solid for 25%). Critical points are presented as large filled circles. The first-order LLPT between LDL and HDL ends in a LLCP (black circle) at $T \simeq 174$ K and $P \simeq 0.13$ GPa for all c . For $c = 2.4\%$ and 25% a new critical point emerges at approximately $T \simeq 168$ K and $P \simeq 0.15$ GPa, above which the first-order LLPT can no longer be detected. Figure adapted from Fig. 1 of Ref. [25]

nanoparticles to the water monolayer we observed a decrease in temperature of the liquid-gas spinodal, and a deformation of the TMD line. The TMD line shifts to lower T for P below 0.14 GPa, and to higher T for P above 0.16 GPa [25]. In addition, we noticed a weakening in the first-order LLPT. In particular, at temperatures below 168 K and pressures above 0.15 GPa, there is only one liquid phase and there is no LLPT between the LDL and HDL.

In Fig. 4, we compare the isobars for water with the MC simulations of the coarse-grained model in the presence of and in the absence of hydrophobic nanoparticles (concentration $c = 25\%$). For the case of $c = 0\%$, we observe sharp discontinuities in density ρ for P above 0.13 GPa, which is consistent with a strong LLPT line that terminates at about 0.13 GPa. On the other hand, water confined in the nanoscopic hydrophobic particle matrix displays smaller discontinuities in density than that of $c = 0\%$ in a pressure region between 0.13 GPa and 0.16 GPa. This observation indicates a weakening in the LLPT. Moreover, the maximum slope of ρ vs. T largely decreases above 0.16 GPa, suggesting that there is no first-order phase transition above 0.16 GPa. This result, together with the fluctuation analysis [25], suggests that in this case, the LLPT is delimited by two critical points: one at $P \simeq 0.13$ GPa and another at $P \simeq 0.15$ GPa (Fig. 3).

A detailed finite-size scaling study of response functions such as compressibility, thermal expansion coefficient, and specific heat [25] confirms the absence of the LLPT at high P above 0.16 GPa. It also shows that even a small number of nanoparticles, $c = 2.4\%$, is sufficient to reproduce the effect of the reduction of the first-order LLPT to a narrow region in both P and ρ with two critical points at high and low pressures (Fig. 3).

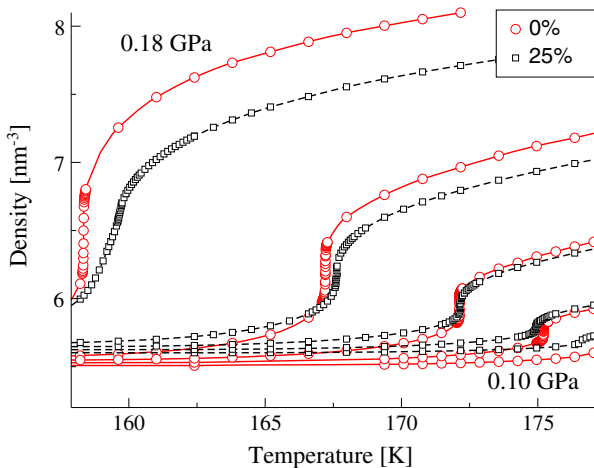


Fig. 4 MC isobars of the coarse-grained model of water with hydrophobic nanoparticles at concentration c , for a system with size $\mathcal{N} = 1.6 \times 10^5$. Isobars are for $P = 0.10$ GPa, 0.12 GPa, 0.14 GPa, 0.16 GPa, and 0.18 GPa (from bottom to top) at $c = 0\%$ (red empty circles with solid connecting lines) and at $c = 25\%$ (black empty squares with dashed connecting lines). At high pressures, isobars for $c = 0\%$ display an infinite slope, which is consistent with a strong LLPT. For the case $c = 25\%$, the maximum slope decreases, which is consistent with the absence of the first-order phase transition

3.2 DMD simulations on mixtures of Jagla ramp potential particles and hard spheres

Several thermodynamic studies employing DMD simulations for bulk Jagla ramp particles have shown a LLPT line that terminates with a LLCP at $T_c = 0.375$, $P_c = 0.243$, and $\rho_c = 0.37$ [51, 52, 94] (see Section 2.2 for the definition of the quantities). The analysis of the isotherms and isochores of the mixtures of Jagla ramp particles and hydrophobic HS solutes with the same size and mass revealed the existence of a LLPT and a LLCP for all mole fractions investigated [44].

Figure 5 shows that when the mole fraction of the HS in the aqueous solution is increased the position of the LLCP shifts to a lower temperature and higher pressure. This shift can occur because the solvation tendency of the HS in the LDL is stronger than that in the HDL [95–98]. We also notice a narrowing of the region in the $P - T$ plane between the LDL and HDL limit of mechanical stability (LMS) as x_{HS} increases, suggesting a weakening of the LLPT line as solute content increases.

The presence of HS narrows the LDL-HDL coexistence envelope in both the $P - T$ and the $P - \rho$ planes. In Fig. 6, the isotherms of bulk Jagla particles are compared to the $x_{\text{HS}} = 0.20$ mixtures. Together with the isochores, the liquid–liquid LMS and the liquid–liquid coexistence line are shown. The LMS line is built by joining the extrema of the isotherms, and the coexistence line is obtained by the Maxwell construction. When going from the bulk case to the $x_{\text{HS}} = 0.20$ case, the width of the regions enclosed by both the coexistence line and the LMS line is reduced, indicating a weaker LLPT. The density anomaly, indicated by the crossing of the isotherms in the $P - \rho$ plane, is well defined in the bulk case, but significantly weaker in the $x_{\text{HS}} = 0.20$ case. The phase diagram of the mixtures changes gradually with concentration (not shown), and while a LLCP with a

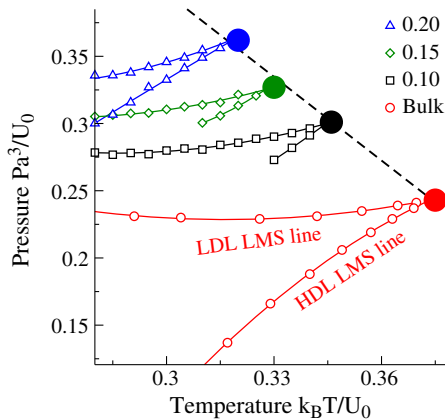


Fig. 5 DMD simulations on the Jagla ramp potential: comparison of the positions of the LLCP (filled circles) upon the increase of the solute mole fractions from 0, or bulk, (red) to $x_{\text{HS}} = 0.10$, 0.15, and 0.20 (in black, green, and blue, respectively). The data points presented with open symbols show the positions of the two branches of the liquid–liquid LMS lines for LDL and HDL (labeled only for bulk, for clarity). Lines connecting the data points are guides for the eyes. Here we observe that upon increasing the solute mole fraction the position of the critical point shifts to lower temperatures and higher pressures and the region enclosed by the LMS lines shrinks. The critical line (dashed) joining the LLCPs of the mixtures is drawn as a guide for the eye. Figure adapted from Fig. 4 of [44]

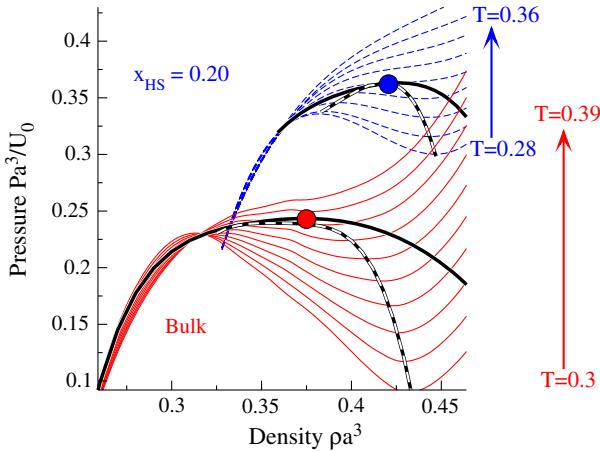


Fig. 6 DMD isotherms for the Jagla potential. Isotherms are shown as fourth-degree polynomial fits to simulated state points in the $P-\rho$ plane for bulk (red solid lines from $T = 0.3$ to 0.39 with a step of $\Delta T = 0.01$) and $x_{\text{HS}} = 0.20$ solution of HS (blue dashed lines from $T = 0.28$ to 0.36 with a step of $\Delta T = 0.01$). The liquid-liquid LMS lines are outlined by striped curves, and the coexistence regions by thick black curves. In the case of the mixture, the LMS density range is reduced in ρ with respect to the bulk case. The LLCs are shown as large filled circles. Density anomaly manifests by crossing of the isotherms in the low-density region. This isothermal crossing is very well pronounced in the bulk case and is significantly weaker in the case of the $x_{\text{HS}} = 0.20$ solution. Figure adapted from Fig. 3 of [44]

narrower coexistence envelope is apparent up to $x_{\text{HS}} = 0.50$, the density anomaly disappears at the highest mole fraction, $x_{\text{HS}} = 0.50$.

4 Comparison to other computational and experimental studies

As we have shown in the previous section, the presence of hydrophobic nanoparticles, either as a confining medium or as a solute, can significantly affect the phase diagram of supercooled liquid water. In particular, it affects the behavior of the LLPT and the position of the LLC. Several studies in the past have addressed the thermodynamic behavior of supercooled water in the presence of a hydrophobic environment. Here, we summarize some relevant findings in the literature and compare them to our own results.

Kumar et al. [28, 29] performed MD simulations on a system composed of 512 TIP5P water molecules confined between two smooth walls, mimicking solid paraffin. They observed a 40 K decrease in T in the overall phase diagram of confined water with respect to bulk water. The temperature shift was qualitatively explained as being caused by the absence of HBs between the hydrophobic walls and water molecules, which on average reduced the number of HBs per molecule in the confined water, analogous to the case of bulk water at high temperatures. Due to the shift to lower T , it was not possible to reach the LLPT found in bulk water. However, inflections in $P-\rho$ isotherms were observed, implying the proximity of the system to the LLC. This result shows that the presence of a LLC in water in a hydrophobic confinement is plausible also when using 3D, orientational-dependent water models, in agreement with the results found for the 2D coarse grained model studied with MC simulations [25] (see Section 3.1).

Gallo and Rovere [26] used MD simulation to study the thermodynamic properties of TIP4P water confined in a rigid disordered matrix of hydrophobic soft spheres upon supercooling. Although they also observed a reduction in the average number of HBs, the HB network appeared preserved, in contrast to the case of water confined between hydrophobic plates. Despite the substantial integrity of the network and the small changes found in the structural properties of confined water, significant shifts to higher P and lower T of both the TMD line and the liquid-gas spinodal were found with respect to bulk TIP4P water. The magnitude of the temperature shift is consistent with water confined between hydrophobic plates. The authors suggested a weak dependence of the properties of water on the hydrophobic confining medium. The existence of a TMD line and liquid-gas spinodal in TIP4P water confined in a rigid disordered matrix of hydrophobic objects compares well with the results shown for the MC simulations (see Section 3.1).

Chatterjee and Debenedetti [45] conducted theoretical investigations of the effect of apolar solutes with different strengths of dispersive interactions (solute–solute interactions) on the mixture phase behavior. They compared this to the bulk phase behavior for a model that incorporates the presence of the LLPT line and the LLCPC and found a critical line originating at water’s second critical point for aqueous mixtures. This line extended towards low P and high T as the solute mole fraction was increased, suggesting a possible accessible experimental manifestation of the LLCPC in the deeply supercooled water. The existence of a critical line originating at the LLCPC of water in solution of hydrophobic objects is in agreement with the results found in the DMD simulations on mixtures of Jagla ramp particles and HS [44] (see Section 3.2). The difference in the direction of the shift of the LLCPC in solutions could be due to the presence of dispersive interactions between apolar particles in the Chatterjee and Debenedetti model and/or to the different slope of the liquid–liquid coexistence line, negative in their case, positive in the Jagla model.

Urbic et al. [54] modeled two-dimensional *Mercedes-Benz* water, freely mobile in a rigid disordered matrix of Lennard-Jones disks. They found that the presence of the obstacles induced perturbations in the water structure. They also demonstrated that high disk densities greatly affect the HB network, and cause a reduction in such response functions as compressibility, in agreement with what was observed in the MC 2D coarse grained model [25].

Finally, Zhang et al. [55] reported experimental results of a 17 K shift towards lower T of the TMD line in water confined in the hydrophobic mesoporous material CMK-1-14, which consists of micrometer-sized grains, each with a three-dimensional interconnected bicontinuous pore structure, with an average pore diameter 14Å, at a hydration level of 99% at ambient pressure. They measured the broadening of the thermal expansion coefficient peak in hydrophobic CMK confinement, contrasting with the sharp peak in the hydrophilic confinement in silica MCM mesopores. The reduction of the anomalous properties of water in hydrophobic environments agrees with what was observed both in the MC simulations on the 2D coarse-grained model [25] (see Section 3.1) and in DMD simulations on the Jagla model [44] (see Section 3.2).

In all of these studies, the effect of the hydrophobic confinement is revealed by a shift in $P - T$ of the thermodynamic loci. Furthermore, experiments [55] and simulations [25, 54] reveal a reduction of the fluctuations with respect to the less hydrophobic cases. In particular, this decrease of fluctuations could be relevant even when the hydrophobic nanoparticle concentration is small [25].

We finally remark that the difference in entropy behavior between the Jagla potential and water, and in particular the coarse-grained model of water presented here, should be taken into account when comparing the results, as this is possibly the origin of the different effect

of the hydrophobic confinement on the LLPT. In the isotropic Jagla potential, the LDL phase has a *larger* entropy than the HDL phase and consequently, through the Clausius-Clapeyron equation ($dP/dT = (\Delta S/\Delta V)$), the HDL-LDL coexistence line has a positive slope. In water and in the coarse-grained model presented here, the LDL phase has a *smaller* entropy than the HDL phase, thus the slope of the HDL-LDL coexistence line is negative. In the Jagla potential with hydrophobic solute [44] the entire LLPT shifts to lower T and higher P as the solute molar fraction is increased. On the other hand, for the coarse-grained model of water confined by hydrophobic nanoparticles between hydrophobic walls [25], the LLCP is almost not affected by the increase of the nanoparticle concentration, but the LLPT is weakened, and eventually disappears, at high P .

5 Conclusions

We have reviewed and compared two recent computational works describing the changes in the thermodynamic behavior in the supercooled region of water and in the LLCP phenomenon for water in hydrophobic environments. We have compared these works with previous reports for water in hydrophobic environments in order to give an overview of the modifications in the phase diagram of water at subfreezing temperatures. We have seen that the presence of a hydrophobic environment can significantly alter the thermodynamic properties of water. The reported temperature shifts in water anomalies and critical points, and the weakening of the LLPT as well as its disappearance at high pressures observed in the MC simulation case, are relevant to current biological research. In biological systems, water is often found in contact with hydrophobic objects, and the results shown can play a crucial role in studies of cryopreservation, in which the reduction of volume fluctuations and the inhibition of ice formation can minimize cell damage.

Acknowledgements We thank K. Stokely for discussions. D. C. and P. G. gratefully acknowledge the computational support received from CASPUR, from the INFN-GRID at Roma Tre University and from the Democritos National Simulation Center at SISSA, Trieste. G. F. thanks the Spanish MICINN grant FIS2009-10210 (co-financed FEDER). M. G. M. acknowledges support by the German Research Foundation (DFG) within the framework of the “International Graduate Research Training Group”. S. V. B. acknowledges the partial support of this research through the Dr. Bernard W. Gamson Computational Science Center at Yeshiva College. E. G. S., M. G. M. and H. E. S. acknowledge support by NSF grants CHE0908218 and CHE0911389.

References

1. Debenedetti, P.G.: Supercooled and glassy water. *J. Phys., Condens. Matter* **15**, R1669–R1726 (2003)
2. Franks, F.: *Water: A Matrix for Life*, 2nd edn. Royal Society of Chemistry, Cambridge (2000)
3. Stanley, H.E.: A polychromatic correlated-site percolation problem with possible relevance to the unusual behavior of supercooled H₂O and D₂O. *J. Phys. A* **12**, L329–L337 (1979)
4. Angell, C.A., Sichina, W.J., Oguni, M.: Heat capacity of water at extremes of supercooling and superheating. *J. Phys. Chem.* **86**, 998–1002 (1982)
5. Kell, G.S.: Precise representation of volume properties of water at one atmosphere. *J. Chem. Eng. Data* **12**, 66–69 (1967)
6. Poole, P.H., Sciortino, F., Essmann, U., Stanley, H.E.: Phase behaviour of metastable water. *Nature* **360**, 324–328 (1992)
7. Tanaka, H.: Phase behaviors of supercooled water: reconciling a critical point of amorphous ices with spinodal instability. *J. Chem. Phys.* **105**, 5099–5111 (1996)
8. Poole, P.H., Saika-Voivod, I., Sciortino, F.: Density minimum and liquid-liquid phase transition. *J. Phys., Condens. Matter* **17**, L431–L437 (2005)

9. Harrington, S., Poole, P.H., Sciortino, F., Stanley, H.E.: Equation of state of supercooled SPC/E water. *J. Chem. Phys.* **107**, 7443–7450 (1997)
10. Jedlovsky, P., Vallauri, R.: Liquid-vapor and liquid-liquid phase equilibria of the Brodholt-Sampoli-Vallauri polarizable water model. *J. Chem. Phys.* **122**, 81101 (2005)
11. Paschek, D., Ruppert, A., Geiger, A.: Thermodynamic and structural characterization of the transformation from a metastable low-density to a very high-density form of supercooled TIP4P-Ew model water. *ChemPhysChem* **9**, 2737–2741 (2008)
12. Liu, Y., Panagiotopoulos, A.Z., Debenedetti, P.G.: Low-temperature fluid-phase behavior of ST2 water. *J. Chem. Phys.* **131**, 104508 (2009)
13. Abascal, J.L.F., Vega, C.: Widom line and the liquid-liquid critical point for the TIP4P/2005 water model. *J. Chem. Phys.* **133**, 234502 (2010)
14. Franzese, G., Marqués, M.I., Stanley, H.E.: Intramolecular coupling as a mechanism for a liquid-liquid phase transition. *Phys. Rev. E* **67**, 011103 (2003)
15. Chen, S.-H., Loong, C.K.: Neutron scattering investigations of proton dynamics of water and hydroxyl species in confined geometries. *Nucl. Eng. Technol.* **38**, 201–224 (2006)
16. Liu, D., Zhang, Y., Liu, Y., Wu, J., Chen, C.-C., Mou, C.-Y., Chen, S.-H.: Density measurement of 1-D confined water by small angle neutron scattering method: pore size and hydration level dependences. *J. Phys. Chem B* **112**, 4309–4312 (2008)
17. Mallamace, F., Broccio, M., Corsaro, C., Faraone, A., Liu, L., Mou, C.-Y., Chen, S.-H.: Dynamical properties of confined supercooled water: an NMR study. *J. Phys., Condens. Matter* **18**, S2285–S2297 (2006)
18. Starr, F.W., Nielsen, J.K., Stanley, H.E.: Fast and slow dynamics of hydrogen bonds in liquid water. *Phys. Rev. Lett.* **82**, 2294–2297 (1999)
19. Mallamace, F., Broccio, M., Corsaro, C., Faraone, A., Majolino, D., Venuti, V., Liu, L., Mou, C.-Y., Chen, S.-H.: Evidence of the existence of the low-density liquid phase in supercooled, confined water. *Proc. Natl. Acad. Sci. USA* **104**, 424–428 (2007)
20. Han, S., Kumar, P., Stanley, H.E.: Absence of a diffusion anomaly of water in the direction perpendicular to hydrophobic nanoconfining walls. *Phys. Rev. E* **77**, 030201 (2008)
21. Giovambattista, N., Rossky, P.J., Debenedetti, P.: Effect of pressure on the phase behavior and structure of water confined between nanoscale hydrophobic and hydrophilic plates. *Phys. Rev. E* **73**, 041604 (2006)
22. Giovambattista, N., Debenedetti, P., Rossky, P.J.: Effect of surface polarity on water contact angle and interfacial hydration structure. *J. Phys. Chem. B* **111**, 9581–9587 (2007)
23. Majumder, M., Chopra, N., Andrews, R., Hinds, B.J.: Nanoscale hydrodynamics: enhanced flow in carbon nanotubes. *Nature* **438**, 44 (2005)
24. Joseph, S., Aluru, N.R.: Pumping of confined water in carbon nanotubes by rotation-translation coupling. *Phys. Rev. Lett.* **101**, 064502 (2008)
25. Strelakova, E.G., Mazza, M.G., Stanley, H.E., Franzese, G.: Large decrease of fluctuations for supercooled water in hydrophobic nanoconfinement. *Phys. Rev. Lett.* **106**, 145701 (2011)
26. Gallo, P., Rovere, M.: Structural properties and liquid spinodal of water confined in a hydrophobic environment. *Phys. Rev. E* **76**, 061202 (2007)
27. Gallo, P., Rovere, M., Chen, S.-H.: Dynamic crossover in supercooled confined water: understanding bulk properties through confinement. *J. Phys. Chem. Lett.* **1**, 729–733 (2010)
28. Kumar, P., Buldyrev, S.V., Starr, F.W., Giovambattista, N., Stanley, H.E.: Thermodynamics, structure, and dynamics of water confined between hydrophobic plates. *Phys. Rev. E* **72**, 051503 (2005)
29. Kumar, P., Yan, Z., Xu, L., Mazza, M.G., Buldyrev, S.V., Chen, S.-H., Sastry, S., Stanley, H.E.: Glass transition in biomolecules and the liquid-liquid critical point of water. *Phys. Rev. Lett.* **97**, 177802 (2006)
30. Bellissent-Funel, M.-C., Chen, S.H., Zanotti, J.-M.: Single-particle dynamics of water molecules in confined space. *Phys. Rev. E* **51**, 4558–4569 (1995)
31. Swenson, J., Jansson, H., Bergman, R.: Relaxation processes in supercooled confined water and implications for protein dynamics. *Phys. Rev. Lett.* **96**, 247802 (2006)
32. Mallamace, F., Broccio, M., Corsaro, C., Faraone, A., Wanderlingh, U., Liu, L., Mou, C.-Y., Chen, S. H.: The fragile-to-strong dynamic crossover transition in confined water: nuclear magnetic resonance results. *J. Chem. Phys.* **124**, 161102 (2006)
33. Angell, C.A.: Insights into phases of liquid water from study of its unusual glass-forming properties. *Science* **319**, 582–587 (2008)
34. Pittia, P., Cesàro, A.: Water biophysics: how water interacts with biomolecules. *Food Biophys.* **6**, 183–185 (2011)

35. Oguni, M., Angell, C.A.: Hydrophobic and hydrophilic solute effects on the homogeneous nucleation temperature of ice from aqueous solutions. *J. Phys. Chem.* **87**, 1848–1851 (1983)
36. Corradini, D., Rovere, M., Gallo, P.: A route to explain water anomalies from results on an aqueous solution of salt. *J. Chem. Phys.* **132**, 134508 (2010)
37. Corradini, D., Rovere, M., Gallo P.: Structural properties of high and low density water in a supercooled aqueous solution of salt. *J. Phys. Chem. B* **115**, 1461–1468 (2011)
38. Mishima, O.: Application of polymorphism in water to spontaneous crystallization of emulsified $LiClH_2O$. *J. Chem. Phys.* **123**, 154506 (2005)
39. Mishima, O.: Phase separation in dilute $LiClH_2O$ solution related to the polymorphism of liquid water. *J. Chem. Phys.* **126**, 244507 (2007)
40. Huang, C., Weiss, T.M., Nordlund, D., Wikfeldt, K.T., Pettersson, L.G.M., Nilsson, A.: Increasing correlation length in bulk supercooled H_2O , D_2O , and $NaCl$ solution determined from small angle x-ray scattering. *J. Chem. Phys.* **133**, 134504 (2010)
41. Corradini, D., Gallo, P., Rovere, M.: Thermodynamic behavior and structural properties of an aqueous sodium chloride solution upon supercooling. *J. Chem. Phys.* **128**, 244508 (2008)
42. Corradini, D., Gallo, P., Rovere, M.: Effect of concentration on the thermodynamics of sodium chloride aqueous solutions in the supercooled regime. *J. Chem. Phys.* **130**, 154511 (2009)
43. Corradini, D., Gallo, P., Rovere, M.: Molecular dynamics studies on the thermodynamics of the supercooled sodium chloride aqueous solution at different concentrations. *J. Phys., Condens. Matter* **22**, 284104 (2010)
44. Corradini, D., Buldyrev, S.V., Gallo, P., Stanley, H.E.: Effect of hydrophobic solutes on the liquid-liquid critical point. *Phys. Rev. E* **81** 061504 (2010)
45. Chatterjee, S., Debenedetti, P.G.: Fluid-phase behavior of binary mixtures in which one component can have two critical points. *J. Chem. Phys.* **124**, 154503 (2006)
46. Magno, A., Gallo, P.: Understanding the mechanisms of bioprotection: a comparative study of aqueous solutions of trehalose and maltose upon supercooling. *J. Phys. Chem. Lett.* **2**, 977–982 (2011)
47. Ball, P.: Water as an active constituent in cell biology. *Chem. Rev.* **108**, 74–108 (2008)
48. Ball, P.: *Life's Matrix: A Biography of Water*. Farrar, Straus, and Giroux, New York (2000)
49. Granick, S., Bae S.C.: A curious antipathy for water. *Science* **322**, 1477–1478 (2008)
50. Poole, P.H., Sciortino, F., Essmann, U., Stanley, H.E.: The spinodal of liquid water. *Phys. Rev. E* **48**, 3799–3817 (1993)
51. Xu, L., Kumar, P., Buldyrev, S.V., Chen, S.-H., Poole, P.H., Sciortino, F., Stanley, H.E.: Relation between the Widom line and the dynamic crossover in systems with a liquid-liquid critical point. *Proc. Natl. Acad. Sci. USA* **102**, 16558–16562 (2005)
52. Xu, L., Buldyrev, S.V., Angell, C.A., Stanley, H.E.: Thermodynamics and dynamics of the two-scale spherically symmetric Jagla ramp model of anomalous liquids. *Phys. Rev. E* **74**, 031108 (2006)
53. Stokely, K., Mazza, M.G., Stanley, H.E., Franzese, G.: Effect of hydrogen bond cooperativity on the behavior of water. *Proc. Natl. Acad. Sci. USA* **107**, 1301–1306 (2010)
54. Urbic, T., Vlachy, V., Pizio, O., Dill, K.A.: Water-like fluid in the presence of Lennard-Jones obstacles: predictions of an associative replica Ornstein-Zernike theory. *J. Mol. Liq.* **112**, 71 (2004)
55. Zhang, Y., Liu, K.-H., Lagi, M., Liu, D., Littrell, K.C., Mou, C.-Y., Chen, S.-H.: Absence of the density minimum of supercooled water in hydrophobic confinement. *J. Phys. Chem. B* **113**, 5007 (2009)
56. Cataudella, V., Franzese, G., Nicodemi, M., Scala, A., Coniglio, A.: Percolation and cluster Monte Carlo dynamics for spin models. *Phys. Rev. E* **54**, 175–189 (1996)
57. Franzese, G., Coniglio, A.: Phase transitions in the Potts spin-glass model. *Phys. Rev. E* **58**, 2753–2759 (1998)
58. Wolff, U.: Collective Monte Carlo updating for spin systems. *Phys. Rev. Lett.* **62**, 361–364 (1989)
59. Mazza, M.G., Stokely, K., Pagnotta, S.E., Bruni, F., Stanley, H.E., Franzese, G.: Two dynamic crossovers in protein hydration water. *Proc. Natl. Acad. Sciences* (2011). doi:[10.1073/pnas.1104299108](https://doi.org/10.1073/pnas.1104299108)
60. Mazza, M.G., Stokely, K., Strelakova, E.G., Stanley, H.E., Franzese, G.: Cluster Monte Carlo and numerical mean field analysis for the water liquid-liquid phase transition. *Comput. Phys. Commun.* **180**, 497–502 (2009)
61. Franzese, G., Bianco, V., Iskrov, S.: Water at interface with proteins. *J. Food Biophys.* **6**, 186–198 (2011)
62. Franzese, G., Stanley, H.E.: A theory for discriminating the mechanism responsible for the water density anomaly. *Physica A* **314**, 508–513 (2002)
63. Franzese, G., Stanley, H.E.: Liquid-liquid critical point in a Hamiltonian model for water: analytic solution. *J. Phys., Condens. Matter* **14**, 2201–2209 (2002)
64. Franzese, G., Stanley, H.E.: The Widom line of supercooled water. *J. Phys., Condens. Matter* **19**, 205126 (2007)

65. Kumar, P., Franzese, G., Stanley, H.E.: Predictions of dynamic behavior under pressure for two scenarios to explain water anomalies. *Phys. Rev. Lett.* **100**, 105701 (2008)
66. Kumar, P., Franzese, G., Stanley, H.E.: Dynamics and thermodynamics of water. *J. Phys., Condens. Matter* **20**, 244114 (2008)
67. Franzese, G., de los Santos, F.: Dynamically slow processes in supercooled water confined between hydrophobic plates. *J. Phys., Condens. Matter* **21**, 504107 (2009)
68. Franzese, G., Hernando-Martínez, A., Kumar, P., Mazza, M.G., Stokely, K., Strelakova, E.G., de los Santos, F., Stanley, H.E.: Phase transitions and dynamics of bulk and interfacial water. *J. Phys., Condens. Matter* **22**, 284103 (2010)
69. Franzese, G., Stokely, K., Chu, X.-Q., Kumar, P., Mazza, M.G., Chen, S.-H., Stanley, H.E.: Pressure effects in supercooled water: comparison between a 2D model of water and experiments for surface water on a protein. *J. Phys.: Condens. Matter* **20**, 494210 (2008)
70. Buldyrev, S.V.: Application of discrete molecular dynamics to protein folding and aggregation. *Lect. Notes Phys.* **752**, 97–131 (2008)
71. Canpolat, M., Starr, F.W., Sadr-Lahijany, M.R., Scala, A., Mishima, O., Havlin, S., Stanley, H.E.: Local structural heterogeneities in liquid water under pressure. *Chem. Phys. Lett.* **294**, 9–12 (1998)
72. Sadr-Lahijany, M.R., Scala, A., Buldyrev, S.V., Stanley, H.E.: Liquid state anomalies for the Stell-Hemmer core-softened potential. *Phys. Rev. Lett.* **81**, 4895–4898 (1998)
73. Xu, L., Buldyrev, S.V., Giovambattista, N., Angell, C.A., Stanley, H.E.: A monatomic system with a liquid-liquid critical point and two distinct glassy states. *J. Chem. Phys.* **130**, 054505 (2009)
74. Xu, L., Ehrenberg, I., Buldyrev, S.V., Stanley, H.E.: Relationship between the liquid-liquid phase transition and dynamic behavior in the Jagla model. *J. Phys.: Condens. Matter* **18**, S2239–S2246 (2006)
75. Kumar, P., Buldyrev, S.V., Sciortino, F., Zaccarelli E., Stanley, H.E.: Static and dynamic anomalies in a repulsive spherical ramp liquid: theory and simulation. *Phys. Rev. E* **72**, 021501 (2005)
76. Gibson, H.M., Wilding, N.B.: Metastable liquid-liquid coexistence and density anomalies in a core-softened fluid. *Phys. Rev. E* **73**, 061507 (2006)
77. Lomba, E., Almarza, N.G., Martín, C., McBride, C.: Phase behavior of attractive and repulsive ramp fluids: integral equation and computer simulation studies. *J. Chem. Phys.* **126**, 244510 (2007)
78. Franzese, G., Malescio, G., Skibinsky, A., Buldyrev, S.V., Stanley, H.E.: Generic mechanism for generating a liquid-liquid phase transition. *Nature* **409**, 692–695 (2001)
79. Buldyrev, S.V., Franzese, G., Giovambattista, N., Malescio, G., Sadr-Lahijany, M.R., Scala, A., Skibinsky, A., Stanley, H.E.: Double-step potential models of fluids - Anomalies and a liquid-liquid phase transition. NATO Science Series, series II: Mathematics, Physics and Chemistry (2002)
80. Franzese, G., Malescio, G., Skibinsky, A., Buldyrev, S.V., Stanley, H.E.: Metastable liquid-liquid phase transition in a single-component system with only one crystal phase and no density anomaly. *Phys. Rev. E* **66**, 051206 (2002)
81. Malescio, G., Franzese, G., Pellicane, G., Skibinsky, A., Buldyrev, S.V., Stanley, H.E.: Liquid-liquid phase transition in one-component fluids. *J. Phys., Condens. Matter* **14**, 2193–2200 (2002)
82. Buldyrev, S.V., Franzese, G., Giovambattista, N., Malescio, G., Sadr-Lahijany, M.R., Scala, A., Skibinsky, A., Stanley, H.E.: Models for a liquid-liquid phase transition. *Physica A* **304**, 23–42 (2002)
83. Skibinsky, A., Buldyrev, S.V., Franzese, G., Malescio, G., Stanley, H.E.: Liquid-liquid phase transitions for soft-core attractive potentials. *Phys. Rev. E* **69**, 061206 (2004)
84. Malescio, G., Franzese, G., Skibinsky, A., Buldyrev, S.V., Stanley, H.E.: Liquid-liquid phase transition for an attractive isotropic potential with wide repulsive range. *Phys. Rev. E* **71**, 061504 (2005)
85. Franzese, G.: Differences between discontinuous and continuous soft-core attractive potentials: the appearance of density anomaly. *J. Mol. Liq.* **136**, 267 (2007)
86. de Oliveira, A.B., Franzese, G., Netz, P.A., Barbosa, M.C.: Waterlike hierarchy of anomalies in a continuous spherical shouldered potential. *J. Chem. Phys.* **128**, 064901 (2008)
87. Vilaseca, P., Franzese, G.: Softness dependence of the anomalies for the continuous shouldered well potential. *J. Chem. Phys.* **133**, 084507 (2010)
88. Vilaseca, P., Franzese, G.: Isotropic soft-core potentials with two characteristic length scales and anomalous behaviour. *J. Non-Cryst. Solids* **357**, 419–426 (2011)
89. Jagla, E.A.: Core-softened potentials and the anomalous properties of water. *J. Chem. Phys.* **111**, 8980 (1999)
90. Jagla, E.A.: Phase behavior of a system of particles with core collapse. *Phys. Rev. E* **58**, 1478–1486 (1998)
91. Yan, Z., Buldyrev, S.V., Giovambattista, N., Stanley, H.E.: Structural order for one-scale and two-scale potentials. *Phys. Rev. Lett.* **95**, 130604 (2005)

92. Yan, Z., Buldyrev, S.V., Giovambattista, N., Debenedetti, P.G., Stanley, H.E.: A family of tunable spherically-symmetric potentials that span the range from hard spheres to water-like behavior. *Phys. Rev. E* **73**, 051204 (2006)
93. Yan, Z., Buldyrev, S.V., Kumar, P., Giovambattista, N., Stanley, H.E.: Correspondence between phase diagrams of the TIP5P water model and a spherically symmetric repulsive ramp potential. *Phys. Rev. E* **77**, 042201 (2008)
94. Xu, L., Mallamace, F., Yan, Z., Starr, F.W., Buldyrev, S.V., Stanley, H.E.: Appearance of a fractional Stokes-Einstein relation in water and a structural interpretation of its onset. *Nat. Phys.* **5**, 565–569 (2009)
95. Paschek, D.: How the liquid-liquid transition affects hydrophobic hydration in deeply supercooled water. *Phys. Rev. Lett.* **94**, 217802 (2005)
96. Buldyrev, S.V., Kumar, P., Debenedetti, P.G., Rosky, P., Stanley, H.E.: Water-like solvation thermodynamics in a spherically-symmetric solvent model with two characteristic lengths. *Proc. Natl. Acad. Sci. USA* **104**, 20177–20182 (2007)
97. Buldyrev, S.V., Kumar, P., Sastry, S., Stanley, H.E., Weiner, S.: Hydrophobic collapse and cold denaturation in the Jagla model of water. *J. Phys., Condens. Matter* **22**, 284109 (2010)
98. Stanley, H.E., Buldyrev, S. V., Franzese, G., Kumar, P., Mallamace, F., Mazza, M.G., Stokely, K., Xu, L.: Liquid polymorphism: water in nanoconfined and biological environments. *J. Phys., Condens. Matter* **22**, 284101 (2010)